Hydrol. Earth Syst. Sci. Discuss., https://doi.org/10.5194/hess-2016-355
Manuscript under review for journal Hydrol. Earth Syst. Sci.
Discussion started: 1 August 2017

Hydrology and Earth System Sciences
Open Access
Discussions

Estimating epikarst water storage by time-lapse surface to depth gravity measurements

Cédric Champollion[1], Sabrina Deville[1], Jean Chery[1], Erik Doerflinger[1], Nicolas Le Moigne[1], Roger Bayer[1], Philippe Vernant[1]

[1] *Laboratoire Géosciences Montpellier, Université Montpellier, 34090 Montpellier, France*

Accepted *date*. Received *date*; in original form *date*

Abstract:
In this study we attempt to evaluate the magnitude of epikarstic water storage variation in various karst settings using a relative spring gravimeter. Gravity measurements are performed two times a year at the surface and inside caves at different depths on three karst hydro-systems in southern France: two limestone karst systems and one dolomite karst system. We find that water storage variations occur mainly in the first ten meters of karst unsaturated zone. Afterward, surface to depth gravity measurements are compared between the sites with respect of net water inflow. A difference of seasonal water storage is evidenced probably associated with the lithology. The transmissive function of the epikarst has been partially deduced from the water storage change estimation. Long (> 6 months) and short (< 6 months) transfer time are revealed in the dolomite and in the limestone respectively.

1) Introduction

Despite carbonate karst systems are largely spread in the Mediterranean area, their associated water resources and vulnerability remain poorly known. In a context of climate change and population increase, the karstic areas are becoming key water resources. A better knowledge of the properties of the karst reservoir is therefore needed to manage and protect the resources (Bakalowicz, 2005). Increasing the knowledge of karst hydrogeological properties and functioning is not a simple task. Indeed, a karstified area is complex and spatially heterogeneous with a non-linear response to rainfall. Numerous in-situ field observations lead to the identification of three karst horizons: epikarst, infiltration zone and saturated zone. The epikarst has been first defined by Mangin (1975) as the part of the underground in interaction with the soil and the atmosphere. It is often described as highly altered zone with a large porosity. In many cases, the epikarst is thought to be a significant water reservoir (Lastennet & Mudry, 1997; Perrin et al., 2003; Klimchouk, 2004; Williams, 2008). Chemically based modeling studies suggest that the epikarst could contribute to the total flow discharge at the spring from 30% to 50% (Batiot et al., 2003; Emblanch et al., 2003). This view drastically differs from other studies that attribute most of the discharge to a deeper storage (Mangin, 1975; Fleury et al., 2007). As the epikarst is also vulnerable to potential surface pollution, a better understanding of its hydrological behavior is welcome for an optimal management and protection of water resource and biological activity.

The studies about the karst water transfer and storage use tools generally based on chemical analysis, borehole measurements and spring hydrograph often associated with modeling approach (Pinault et al., 2001; Hu et al., 2008; Zhang et al., 2011). Spring chemistry or flow approaches provide useful information at basin scale however bringing limited clues about the spatial distribution of hydrogeological properties. On the opposite, borehole measurements provide useful quantitative information but relevant only for the near field scale because of the strong medium heterogeneity. At the intermediate scale (~100m), the determination of the hydrogeological karst properties can be reached by geophysical experiments. Therefore, a collection of geophysical observations at intermediate scale can be valuable for constraining distributed modeling studies and more understanding of epikarst processes. Various geophysical tools are used to monitor, at an intermediate scale, transfer and storage properties such as Magnetic Resonance Sounding (MRS) (Legchenko et al. 2002), 4D seismic (Wu et al., 2006; Valois, 2011), Electrical Resistivity Tomography (ERT) (Valois, 2011) and gravity measurements (Van Camp et al., 2006a; Jacob et al., 2010) among others. Both distributed geophysical measurements (ERT, 4D seismic) and integrative methods (MRS, gravity) revealed spatial variations associated to medium heterogeneities.

Gravity methods are nowadays pertinent tools for hydrogeological studies in various contexts (Van Camp et al., 2006a; Davis et al., 2008). The value of the gravity at Earth surface is indeed directly influenced by underground rock density. A variation of density due to water

Hydrol. Earth Syst. Sci. Discuss., https://doi.org/10.5194/hess-2016-355
Manuscript under review for journal Hydrol. Earth Syst. Sci.
Discussion started: 1 August 2017

saturation at depth can be directly measured from the surface through the temporal variation of the gravity (Harnisch & Harnisch, 2006; Van Camp et al., 2006b). Modern and accurate ground-based gravimeters provide a direct measurement of the temporal water storage changes in the underground without the need of any complementary petrophysic relationship (Davis et al., 2008; Jacob et al., 2008; Jacob et al., 2010). Time-lapse gravity measurements stand as an efficient hydrological tool for the estimation of water storage variations in both saturated and unsaturated zone. Moreover, the sampling volume of the gravity is increasing with depth: at 10 meters depth, the gravity integrates over a surface of about 100*100 m averaging small scale variability. As surface gravity measurement integrates all density changes above the gravimeter, observed temporal variations can be related to both saturated and unsaturated zones. Time-lapse surface gravity measurements alone provide poor information about the vertical distribution of water. To get around the absence of vertical resolution, gravity measurement can be done at different depths in caves or tunnels (Jacob et al., 2009). Such time-lapse Surface to Depth (S2D) gravity measurement allows estimating water storage variations in the unsaturated zone of the karst. Previous studies of gravity S2D measurements made in natural cave suggest that water storage variations in the epikarst can be a major part of total water storage changes across the aquifer (Jacob et al., 2009). In the present study, we use gravity data to quantify the influence of the epikarst in term of seasonal water storage in two karst systems in the south of France. We first present the hydrogeological situation of the sites and the experimental setup are introduced. Then the gravity data processing is detailed and results are presented. Results from another site in neighboring area (Jacob et al., 2009) are recalled and discussed in comparison with the results from the additional sites survey. Subsequently, time-lapse S2D gravity variations are analyzed in the light of these depth distributions. Finally, the seasonal water storage for all sites is discussed in terms of processes during the recharge and discharge of the epikarst and its link with lithology.

1) Hydrogeological setting of studied karst systems

a) Lamalou karst system (SEOU site)

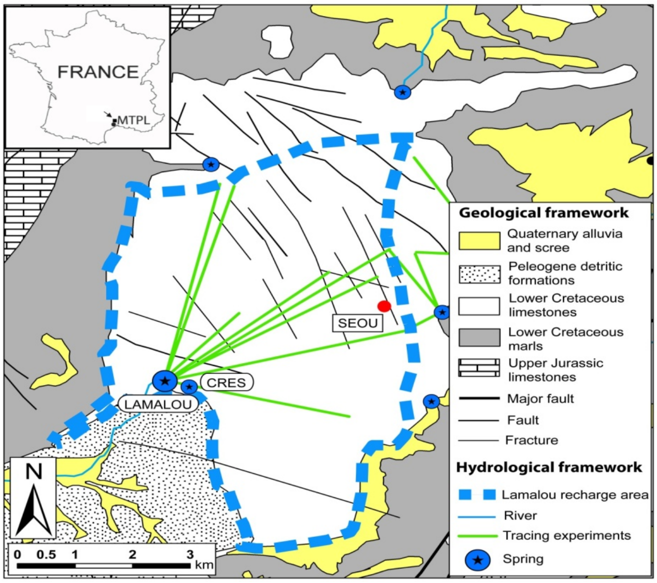

Figure 1 : a) Hydrogeological setting of Lamalou karst system on the Hortus plateau. Seoubio cave (SEOU) is indicated by a red dot;

The Lamalou karst system is located on the Hortus plateau (South of France). The aquifer is set in 100 m thick formation of lower Cretaceous compact limestone (Figure 1) deposited on Berriasian marls formation. These marls act as an impermeable barrier and define the lower limits of the saturated zone. Tertiary deposits overhang Cretaceous formations at the south-west and limit the aquifer. The karstified limestone formation is weakly folded as a NE-SW synclinal structure linked to Pyrenean compression. The main recharge of the Lamalou karst system comes from rainfall which annually reaches 900 mm. Snow occurs less than once a year and is negligible in the seasonal water cycle. Surface runoff is extremely rare except during high precipitation events when most of the system is saturated (Boinet, 1999). Discharge of Lamalou karst system only occurs at perennial Lamalou-Crès springs system composed of two perennial springs connected during high flow period (Durand, 1992). Daily discharge is 5 l/s and 1.5 l/s respectively for Lamalou spring and Crès spring (Chevalier, 1988). From combination of geomorphological observations, tracing experiments and mass balance modeling, the Lamalou recharge area is estimated of ~30 km² (Bonnet et al., 1980; Chevalier, 1988). The vadose zone has a maximum thickness of ~45m. The epikarst thickness is estimated to 10 – 12 m depth at spring vicinity (Al-fares et al., 2002) and corresponds to an altered limestone with a strong secondary porosity such as opened fractures.

Hydrol. Earth Syst. Sci. Discuss., https://doi.org/10.5194/hess-2016-355
Manuscript under review for journal Hydrol. Earth Syst. Sci.
Discussion started: 1 August 2017

The Lamalou experimental site is a cave called Seoubio (SEOU) located to the North-East part of the system in Valanginian limestone (Figure 1). The surface topography is nearly flat around the cave entrance, which corresponds to a vertical pothole of 5 m diameter and 30 m depth allowing a straight descent through the epikarst (Figure 3a). The depth of saturated zone is 39 m below surface as attested by two siphons. The neighboring landscape is made of a 'lapiaz' structure with opened fractures and a very thin soil. The land use around the site is a natural typical Mediterranean scrubland.

b) Gourneyras karst system (BESS site)

The Gourneyras karst system is located in the southern part of Grands Causses area (south of France). The aquifer is set in Middle to Upper Jurassic limestone and dolomite topping Liassic marls formation. The latter formation defines the lower limit of the saturated zone of the karst system. The main recharge of the system comes from rainfall which reaches ~1100 mm annually. The rare snowfalls are included in the precipitation measurements. Discharge occurs only at the Gourneyras Vauclusian-type perennial spring. Discharge is not continuously monitored but punctual measurements suggest a discharge of ~20m^3/s during flood events. Recharge area of Gourneyras spring is estimated to ~41 km² (SIE Rhône-Méditerranée, 2011). The vadose zone has a maximum thickness of 450 m. Fractures plugged with calcite are seen in the cave.

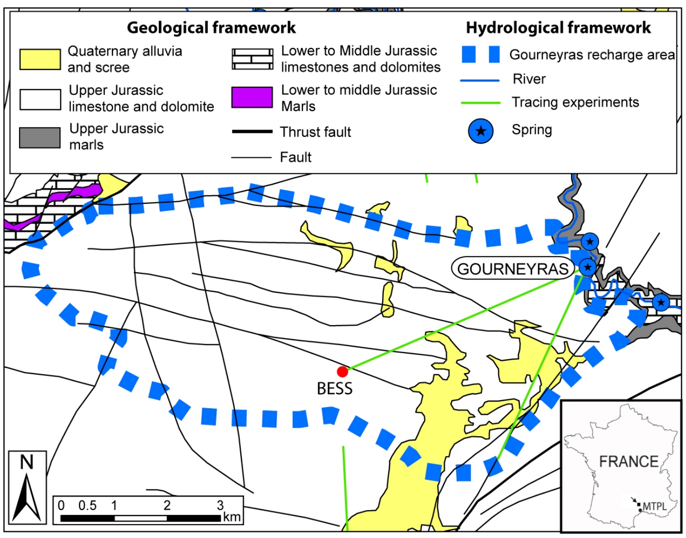

Figure 2 : Hydrogeological location map of Gourneyras karst system. Besses cave is indicated by a red dot (BESS)

Hydrol. Earth Syst. Sci. Discuss., https://doi.org/10.5194/hess-2016-355
Manuscript under review for journal Hydrol. Earth Syst. Sci.
Discussion started: 1 August 2017

The Gourneyras experimental site is a cave called "Les Besses" (BESS) (Figure 2). The surface topography around the cave entrance is a gentle slope to the south-east. The cave is located in Kimmeridgian limestone formations. At the cave location, limestone is overhead by a thin dolomite formation. Shallow alteration deposits such as clay are present at the surface. Above the cave, the land use is a natural typical Mediterranean scrubland. The cave morphology allows an easy afoot descent except between 670 m and 690 m elevation where abseiling rope is necessary. The cave topography allowed us taking gravity measurements at 5 different depths (Figure 3b). Saturated zone is probably at 450m depth below the surface a few tenths of meters above spring elevation.

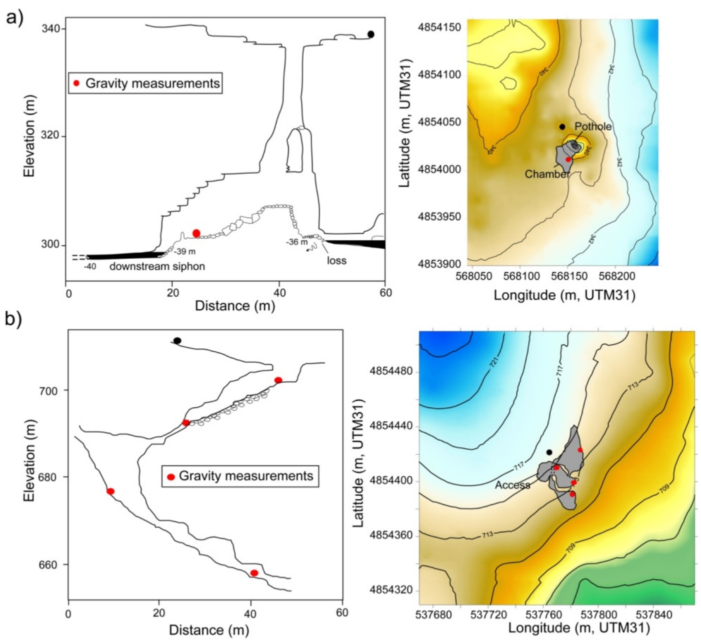

Figure 3: Developed cross-section and topography surrounding a) Seoubio caves, after Boinet (2002); and b) Besses caves. Black and red circles indicate the location of gravity measurements. Elevations are in meters. The projections of the cave in surface are represented in gray on topography.

The two karst systems of SEOU and BESS sites have been presented above but the results from a previous study (Jacob et al., 2009) are extensively used in the discussion (BEAU site). A detailed description of the site BEAU is available in Jacob et al. (2009). BEAU and BESS sites are located 25 km away at the same elevation with a similar geological and climatic setting. However, the BEAU site is embedded in a highly altered dolomite capped with a shallow soil of the Durzon karst hydro-system.

2) Data acquisition and processing

a) Cave topography

Positions of cave gravity stations at each site were measured using standard speleologists tools. Azimuth, inclination and distance measurements were performed along 2 topographic surveys between surface and depth stations. The closing misfit between these surveys indicates an elevation accuracy of about 0.2 m.

b) Meteorological data

Precipitation and potential evapotranspiration are provided by the French national meteorological agency (Météo-France). The nearest meteorological station of each site was selected. Precipitations are daily monitored respectively at 4 km to the South-East of SEOU site and 5km to the South of BESS site. Rain gauges are automatic tipping-bucket with a resolution of 0.2 mm. Accuracy of rain gauges is equal to 4% during weak precipitation, but the errors increase when precipitation exceeds 150 mm/h (10% accuracy) (Civiate & Mandel, 2008) which is rare in the area. Daily potential evapotranspiration (PET_d) is calculated using Pennman-Monteith's formula by Météo-France. PET_d is given at respectively 7 km to the south-west of SEOU site and 5 km to the south of BESS site. The actual evapotranspiration *(AET)* has been calculated from the potential evapotranspiration (PET_d) and a crop coefficient (k). The crop coefficient is time-variable (i.e. during a season) (Allen et al., 1998) and includes effects of water availability and physiological properties of plants. The seasonal variation of the crop coefficient cannot be evaluated without direct monitoring of actual evapotranspiration but a mean yearly value of the crop coefficient can be estimated using yearly actual evapotranspiration (AET_y) and daily potential evapotranspiration (PET_d). Turc's formula gives the AET_y as function of yearly rainfall and yearly mean air temperature (Turc, 1961; Réméniéras, 1986). Yearly average of the crop coefficient (k) is the ratio between AET_y and yearly total PET_d:

$$k=\frac{AET_y}{\sum_{i=1}^{365} PET_d(i)}$$

Based on 12 and 5 years depending on site, the crop coefficient was found equal to 0.51 and 0.49 respectively for SEOU and BESS site. The crop coefficient on the BEAU site in the Durzon karst hydro-system (climate and land use similar to the BESS and SEOU site) has been calculated using different methods and ranges between 0.5 and 0.7 (Jacob, 2009). A

Hydrol. Earth Syst. Sci. Discuss., https://doi.org/10.5194/hess-2016-355
Manuscript under review for journal Hydrol. Earth Syst. Sci.
Discussion started: 1 August 2017

Hydrology and Earth System Sciences
Open Access
Discussions

value of 0.6 for BEAU site has been selected. Due to the lack of realistic error estimation, accuracy of AET is fixed to 15% based on recent estimation of AET from flux tower measurements (Fores et al., 2017). As the AET is much smaller during winter than during summer, the AET uncertainty is higher during the discharge period but allows more confident interpretation during the recharge period.

c) Surface to depth gravity experiment

Experimental setup

The surface to depth (S2D) gravity experiment consists in measuring the time-lapse gravity difference between surface and depth at a given site. S2D was used in previous study in cave about 25 km NW from BESS (Jacob et al., 2009). The morphology of the caves allows taking measurements in the interior of karst and at different depths in the unsaturated zone. For each karst system we choose one cave where the surface and the underground access can be managed with a relative gravimeter. S2D gravity measurements are done at the surface and ~-35m depth at the SEOU cave. For BESS cave, gravity stations are located throughout the cave at different depths: the surface, -12m, -23m, -41m and -53m. To limit temporal bias linked to gravimeter position, the height and orientation of the CG-5 gravity sensor are fixed for all stations using a brass ring positioned on carved holes in the basement rock.

Gravity measurements have been done during at least two years (2010-2011) in late summer and early spring in order to catch the seasonal water cycle. When more than two measurements per year have been done, all the results are averaged at a bi-annual frequency.

Scintrex relative gravimeter CG5 has been used as in previous studies for precise micro-gravity survey (Bonvalot et al., 2008; Merlet et al., 2008; Jacob et al., 2010; Pfeffer et al., 2013). The gravity sensor is based on a capacitive transducer electrostatic feedback system to counteract displacements of a proof mass attached to a fused quartz spring. The CG-5 instrument has a reading resolution of 1 µGal and a repeatability smaller than 10 µGal (Scintrex limited, 2006). The compactness and the accuracy of the gravimeter match the requirements of micro-gravity in natural caves. As gravity signals of hydrological processes display relatively small variations of 10-30 µgal, a careful survey strategy and processing must be applied to gravity data. Relative gravity measurements also need to be corrected for calibration and instrumental drift. We used only the CG-5#167 for the measurements because of its known low drift.

Gravity data processing and error estimation

As demonstrated by Budetta & Carbonne (1997), Scintrex relative gravimeters need to be regularly calibrated when used to detect small gravity variations over extended periods of time. The calibration factor was measured before each gravity period at the Montpellier-Aigoual calibration line (Jacob, 2009). The accuracy of the calibration is 10^{-4}. Calibration

Hydrol. Earth Syst. Sci. Discuss., https://doi.org/10.5194/hess-2016-355
Manuscript under review for journal Hydrol. Earth Syst. Sci.
Discussion started: 1 August 2017

Hydrology and Earth System Sciences
Open Access
EGU
Discussions

factor of CG-5#167 is stable during the studied period. The error of the calibration factor change is therefore negligible.

The gravity data are corrected for Earth tides using ETGTAB software (Wenzel, 1996) with the Tamura tidal potential development (Tamura, 1987). Considering the distance of Atlantic Ocean, the ocean loading effects are weak (6 µGal) and have been removed using Schwiderski tide model (Schwiderski, 1980). Atmospheric pressure loading is corrected using a classical empirical admittance value of -0.3 µGal/hPa (pressure measurements have an accuracy of about 1 hPa with a small field barometer). Polar motion effects are not corrected because they are nearly constant over the time span of one S2D measurement (~ 8 hours).

The drift of the CG-5 sensor is linked to a creep of the quartz spring and must be accurately corrected for obtaining reliable values of gravity variation. The instrumental drift is assumed to be linear during the short time span of the loops (less than one day). The linear drift can be evaluated with repeating measurements at the same station during a day. The drift of the CG5#167 gravimeter is known to be particularly small (Jacob et al., 2009; Jacob et al., 2010).

The gravity differences relative to the reference station and the drift value are obtained using a least-square adjustment scheme. We consider that the effects of temperature change on gravity variations are uncorrelated with the drift. Software MCGRAVI (Belin, 2006) based on the inversion scheme of GRAVNET (Hwang et al., 2002) is used to adjust gravity measurements and drift. Unknowns to be adjusted are gravity value at each station (surface and depths) and the linear drift of the gravimeter. Measurements of one station (m_d) relative to the reference station (m_s) can be expressed as:

$$C_f\left(m_s^{t_j} - m_d^{t_i}\right) + v_{S_i}^{S_j} = g_s - g_d + D_k\left(t_j - t_i\right) \qquad (1)$$

Where C_f is the calibration correction factor, m_s^{tj} and m_d^{ti} respectively the reference and station gravity reading at time t_j and t_i, v_{Si}^{Sj} the residuals of (m_s^{tj} - m_d^{ti}), D_k the linear drift of the loop k, g_s and g_d the gravity values at the reference and the station. The variance of one gravity reading is given by the standard deviation of 90s measurements series and additional errors of 2 µGal for inaccurate gravity corrections and possible setup errors. The a-posteriori variance of unit weight is computed as:

$$\sigma_0^2 = \frac{V^T PV}{n - (m+s)} \qquad (2)$$

Where n is the number of gravity station, s the number of loops, m the number of gravity reading, V is an n vector of residuals and P is a weight matrix. The table 1 summarizes the results of the gravity experiments at each site. One can note that gravity errors budget is always smaller than the measured gravity variations validating the survey setup and processing.

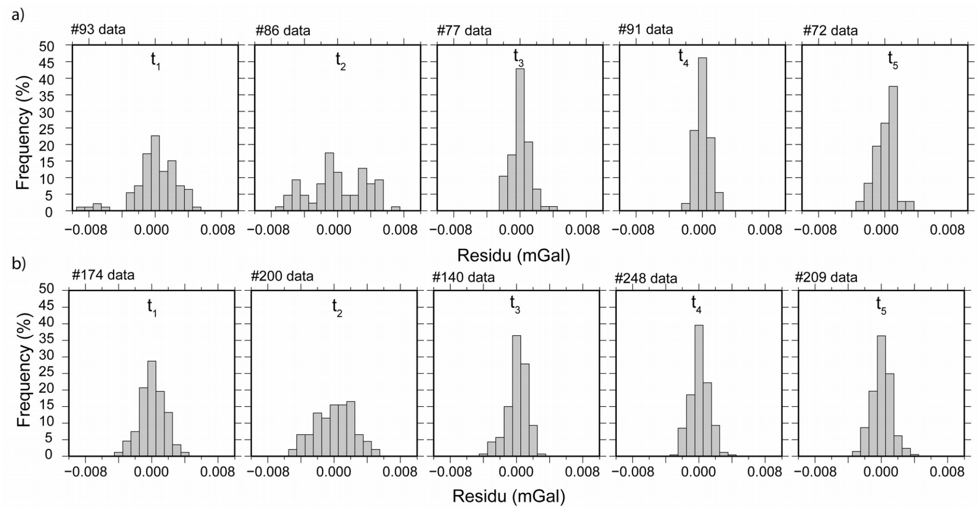

Figure 4 : Histogram of residuals of the fit at a) SEOU site, and b) BESS site for each measurements periods.

Measurement relaxation and measurement strategy

In addition to the daily drift, the transport of the gravimeter causes a relaxation of the quartz spring that leads to a rapid variation of the gravity value during the first ~40 minutes of measurements (in our case for the CG-5 #167). Such a relaxation has been already related in previous studies such as Flury et al. (2007). The relaxation may sometimes be greater than the daily drift of the gravimeter and displays variable amplitude depending probably on time transport and meteorological variations. Contrary to the drift, reasons of the relaxation are not clearly understood and cannot be modeled. Without the correction of the relaxation, the relative gravity measurements lack a clear error budget. To resolve this problem, we setup a new measurement strategy which allowed removing relaxation and we compare it with a usual gravity measurements strategy.

Two measurement strategies are used in this study. The usual one, called “short time strategy” consists to measure at the reference station and the other stations many times (4 and 5 in our case). For each single occupation, 10 measurements of 90s at 6Hz sampling are performed. Only the last 5 or 6 nearly constant measurements are selected. Frequent reference station measurements allow for constraining the instrumental drift and the number of occupations leads to a statistical decrease of the error. With the short time strategy, one assumes that the relaxation due to the transport always results to the same bias from site to site. The time of transportation between two stations is keep as constant as possible to obtain similar relaxation bias. This strategy was used for the two first measurements campaigns (winter 2010 and summer 2010).

The new strategy, called "long time strategy" aims to overcome the relaxation phenomena and is used for the three last measurements campaigns. Only two or three occupations at the reference station and only one at the other stations are done. For each occupation, a minimum of 40 measurements of 90 seconds at 6 Hz sampling are performed (~ 1 hour). The duration is carefully chosen: the relaxation of the gravimeter must be achieved. The gravity reading then follows the daily linear drift. A minimum of 20 gravity reading during the linear, stable measurement period are kept. Such a strategy can be applied only if the drift of the gravimeter is small and linear, which is the case of CG-5#167.

The evaluation of the measurement accuracy can be partially done with the help of the residuals. The residuals are the differences between the measured gravity value and the estimated gravity value. The residuals depend on the accuracy of the processed data and on the robustness of measurements strategy. For example, if a histogram of residual is centered on 0 then it let think that correction process have not introduced a bias in gravity value. The dispersion of the residuals can indicate noisy measurements or non-linear drift. The shape of the histogram shows the global accuracy of dataset. The residuals were estimated for each dataset (Figure 4) and can be used to compare the two measurement strategies.

Most of the histograms display a Gaussian shape centered on zero with a small dispersion showing the good quality of the gravity readings and hence the robustness of the surface to depth gravity differences (Δg_{S2D}). However, the residuals of -8 µGal (Figure 4a) for the period t_1 at SEOU site are due to an unexpected gravity jump during the survey. As no explanation was found for the gravity jump, they are kept for data adjustment even if the dispersion of the gravity residuals increases accordingly. For the two first datasets, Gaussian shapes are observed and 90% of residuals are comprised in 8µGal interval. For the three last datasets, 90% of residuals are between -2µGal and +2µGal. The "long time strategy" reduces the errors of the corrected gravity value. Indeed, residuals histograms of the "long time strategy" are narrower than those of the "short time strategy" which confirms the improvement of the field experiment strategy (Figure 4). We have tested in a cave the "long time strategy" using repeated measurement on a single station interrupted by hand transportation. As for the data shown here, these unpublished results, show a smaller dispersion of the residuals than the one provided by the "short time" method.

All raw gravity data are presented in the Annex 1. For SEOU site, the Δg_{S2D} values show significant temporal variations ranging from -3.897 mGal to -3.914 mGal (annex 1). At BESS site, between surface to 12m depth, Δg_{S2D} values is ranging from -1.523 mGal to -1.537 mGal;

Hydrol. Earth Syst. Sci. Discuss., https://doi.org/10.5194/hess-2016-355
Manuscript under review for journal Hydrol. Earth Syst. Sci.
Discussion started: 1 August 2017

from 12m to 23m depth, Δg_{S2D} show a weak variation and the values ranged between -1.317mGal and -1.322 mGal; for the two latest depths, Δg_{S2D} have no significant variations of -1.724 mGal to -1.728 mGal and -1.272 mGal to -1.277 mGal respectively for 23 to 41m and for 41 to 58m depth intervals. See annex 1 for more details.

3) Data interpretation

Surface to Depth formulation

The ***ΔgS2D*** gravity values contain the variations associated to elevation and to the differential attraction of rocks masses. These time independent effects must be removed for accessing to water storage variations. In the following we assume that the sedimentary formations between the two measurement sites have no lateral variations of density. Let g_s and g_d be the gravity value respectively at the surface and at depth at heights z_s and z_d.

The surface and depth gravity measurements g_s and g_d can be expressed as (Jacob et al., 2009):

$$g_s = 2\pi G \rho_{app} h + 2\pi G \rho_{app} z_s + T_S + z_s \, grad(g_0) + \Delta g_B(z_S) + g_0(\phi_S) + g_{LW}^{S} \quad (3)$$

$$g_d = -2\pi G \rho_{app} h + 2\pi G \rho_{app} z_d + T_d + z_d \, grad(g_0) + \Delta g_B(z_d) + g_0(\phi_d) + g_{LW}^{d} \quad (4)$$

Where (all parameters in SI units) G is the universal gravitational constant, h is the height difference between two stations, ρ_{app} the apparent density of the rock mass below depth station, T_S and T_d the terrain effects at the surface and depth, $grad(g_0)$ the vertical normal gravity gradient known as free-air gradient, Δg_b the Bouguer anomaly, g_0 the normal gravity for surface and depth station at latitude φ_S and φ_D. Additional terms g^{S}_{LW} and g^{d}_{LW} are the long wavelength effects of global hydrology which are dominated by surface deformation induced by hydrological continental loading. At the spatial scale of a few tenths of meters that we consider, the vertical deformation induced by regional hydrological loading is supposed constant. The surface to depth gravity difference can therefore be expressed as:

$$\Delta g_{S2D} = 4\pi G \rho_{app} h + \Delta_z T + h \, grad(g_0) + \Delta_z g_B + \Delta_z g_0(\phi) \quad (5)$$

Where $\Delta_z T$ is the difference of terrain effects between surface and depth station, $\Delta_z g_B$ the difference of Bouguer anomaly between surface and depth station, $\Delta_z g_0(\varphi)$ the change in gravity due to latitude difference between surface and depth station.

Seasonal water storage variations from time-lapse S2D

Once surface to depth gravity differences are calculated, looking at temporal variations allows for retrieving the water storage variations. Time-lapse S2D gravity can be interpreted in term

Hydrol. Earth Syst. Sci. Discuss., https://doi.org/10.5194/hess-2016-355
Manuscript under review for journal Hydrol. Earth Syst. Sci.
Discussion started: 1 August 2017

Hydrology and Earth System Sciences
Open Access
Discussions

of equivalent water height changes, assuming that the water storage variations are laterally homogenous at investigated temporal (seasonal) and spatial (~100 m) scales. Such hypothesis is likely to be untrue in a karstic area because voids and heterogeneities are potentially present at all scales. Looking at a temporal snapshot of the total water storage (porosity time's saturation) in the first meters of the karst should probably show a high heterogeneity as seen in boreholes. Nevertheless, we justify our working hypothesis as follows:

- ✓ S2D gravity measures at an *intermediate (100 m) scale.* The laterally integrative property of the gravity leads to ignore small scale (up to a few meters) heterogeneities which is one of the main advantage of the gravity method. Moreover, the large scale heterogeneities (> 100 m) are negligible because of the differences between surface and depth.
- ✓ Time-lapse S2D gravity measures underground water variations associated to a *seasonal water cycle.* At the seasonal time-scale, the capacitive function of the karst is probably largely dominant and the transfer function as the fast transfer is not measured.
- ✓ Time-lapse S2D gravity measures the average water storage *variations* (i.e. porosity time's saturation variations). As in our case the epikarst is never completely saturated during the measurements, the heterogeneity of the water storage variations is likely to be associated to saturation variation and not to porosity.

Taking into account previous hypothesis, the time variations of each term of equation 5 can be evaluated. The free-air gradient, normal gravity and depth are constant with time because of the absence of tectonic activity. For the duration of investigation, the effects of erosion on topography, caves and potential tectonic activity can be considered as negligible for all sites. Therefore, we can consider topography variations around sites and caves volumes constant with time. Additionally, apparent density variations due to water storage variations yield a negligible influence on terrain effects (<1µGal). Hence, the evolution of surface to depth gravity with time can be reduced to:

$$\Delta_z^t g = 4\pi G \, \Delta_z^{\delta t} \rho_{app} h \qquad (6)$$

Where $\Delta^t\rho_{app}$ is the apparent density change over time t. Surface to depth gravity variations during time period $\Delta_z^t g$ correspond to twice the Bouguer attraction of a plate with $\Delta^t\rho_{app}$ density of height h and therefore increases the signal to noise ratio. Finally, the apparent density variations depend only on water saturation variations. Time-lapse water saturation variation can be approximated to an equivalent water height (EqW) variation (eq. 7). Let $\Delta^t{}_z l$ be the equivalent water layer height variations over time t within height h. Eq 7 induces the

Hydrol. Earth Syst. Sci. Discuss., https://doi.org/10.5194/hess-2016-355
Manuscript under review for journal Hydrol. Earth Syst. Sci.
Discussion started: 1 August 2017

density change $\Delta^t\rho_{app}$. Finally, the time-evolution of $\Delta^t_z g$ can be expressed in the following manner:

$$\Delta_z^t g = 4\pi G \rho_w \Delta_z^t l \quad (7)$$

where ρ_w is density of water. Therefore, a S2D gravity variation of 1µgal is associated to an effective water slab of 23.3 mm.

Site	Time period	Gravity difference (µGal)	Equiv. Water height (EqW) (mm)	Cumulative precipitation (mm)	Cumulative AET (mm)	Net water inflow (NWI) (mm)
SEOU	Feb10-Aug10	-8.5 ± 1.9	-203 ± 48	281 ± 11	239 ± 48	41 ± 49
	Aug10-May11	4.0 ± 1.9	95 ± 48	628 ± 25	254 ± 51	373 ± 56
	May11-Sep11	-1.5 ± 1.0	-35 ± 25	256 ± 10	344 ± 69	-88 ± 69
BESS	Feb10-Aug10	-6.0 ± 3.3	-143 ± 40	315 ± 13	381 ± 76	-66.6 ± 77
	Aug10-May11	5.0 ± 3.3	119 ± 40	854 ± 34	266 ± 53	587 ± 63
	May11-Sep11	-5.5 ± 2.2	-131 ± 33	162 ± 6	320 ± 64	-158 ± 64
BEAU	Sep06-Nov06	13.0 ± 1.1	325 ± 53	445 ± 18	69 ± 14	375 ± 22
	Nov06-Sep07	-10.5 ± 1.7	-262 ± 82	482 ± 19	753 ± 150	-271 ± 151
	Sep07-Feb08	13.0 ± 1.6	325 ± 79	424 ± 17	208 ± 17	217 ± 44

Table 1: Time-lapse S2D gravity difference, Equivalent water height, cumulative precipitation, cumulative evapotranspiration and total water inflow with the associated errors at SEOU, BESS and BEAU site for different recharge and discharge periods.

Results of the time-lapse gravity difference and associated equivalent water height are presented for each site between two consecutive periods (Table 1). Results of BESS and SEOU site are compared to the ones obtained at the BEAU site. As the measurements are done approximately every 6 months during the optimum of the seasonal water cycle, the yearly cycle is measured without ambiguity. Gravity differences from all depths have been added for BESS site to obtain a total EqW. Error budget of EqW is retrieved from S2D gravity standard deviation.

During all discharge periods, gravity differences are negative in the three sites indicating a decrease of EqW. For all recharge periods, gravity differences are always positive indicating an increase of EqW. At SEOU site, the two dry seasons lead to a loss of about 203 mm and 36 mm EqW respectively for first and second discharge period. During recharge period, increase of EqW is equal to 95 mm, in accordance with high precipitation value during this period. At BESS site, the two discharge periods show a similar loss around 131 mm in spite of large precipitation variations. Recharge period has a positive EqW equal to 119 mm with the respect of high precipitation value. At BEAU site, only one discharge period was monitored and the loss is equal to 262 mm. For the two recharge periods EqW have the same value of 325 mm with similar cumulative precipitation. Contrary to the two first sites, cumulative precipitation have a similar values whatever recharge or discharge period, but cumulative AET shows a significant variation with time period. Except for the first recharge period at the SEOU site, the EqW during recharge and during discharge are equivalent.

Epikarst water storage

As the precipitation and the evapotranspiration vary geographically from site to site, EqW cannot be directly compared. Looking to the ratio between the time-lapse S2D gravity variations (or EqW) and the net water inflow allows the inter-comparison between different sites and the interpretation in terms of water storage capacities. The normalization of EqW by the net water inflow allows also comparing EqW measured at other period such as at BEAU site in 2007-2008. No surface runoff has been observed at the three sites even after heavy rainfall. We then consider that all rainfall directly infiltrate into soil. As AET contribute to take out water to the soil, it was taking into account in mass balance. The effective precipitation or the net water inflow (NWI) during a time period is the difference between the cumulative precipitation (P_c) and the cumulative actual evapotranspiration (AET_c) for the given site:

$$NWI = P_c - AET_c \qquad (8)$$

The net water inflow exhibits as expected a seasonal cycle. High values (up to 600 mm) during the recharge and small or negative value during the discharge (up to -263 mm) have been recorded (Table 1).

During the discharge period, EqW and NWI are all negative except for 2010 in SEOU where NWI is equal to 41 mm (a possible explanation is presented later in the section 4. interpretation). The EqW is larger than NWI for the February 2010 to August 2010 discharge period at SEOU and BESS site. On the opposite, for May 2011 to September 2011 discharge period, EqW is lower than NWI (Table 1). At BEAU site, EqW are sometimes larger and sometimes lower than NWI during the discharge. Such unrelated relationship between EqW variations and NWI seems to be typical of the discharge and prevent simple interpretation. The discharge is also characterized by a high error budget of NWI value as the evaluation of AET is dependent of the relative low accuracy of k coefficient. As the AET is important during the discharge, the uncertainty of AET prevents further interpretation. The discharge period is therefore not included in the following discussion.

During the recharge, the two sites BESS and SEOU exhibit a similar pattern as the EqW is always smaller (about three times) than the net water inflow (Figure 5). For example, at BESS site EqW is equal to 119 mm when the net water inflow reaches 587 mm. During the similar season, BEAU exhibits a different pattern with an EqW equivalent to the NWI. We obtain 325mm of EqW with 376mm for NWI. Looking to the year 2011 for SEOU site, EqW corresponds to 30% of net water inflow. For BESS site, the EqW/NWI ratio is equivalent to SEOU site (~30%). On the opposite, EqW/NWI ratio is of about 80% at BEAU site. As the EqW/NWI ratio is a climatic normalization of the seasonal water storage, the heterogeneity in the seasonal water storage is therefore clearly shown as expected in a karstic environment.

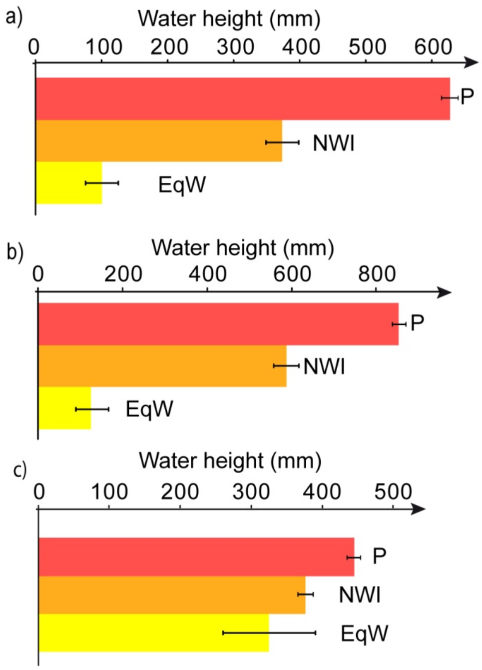

Figure 5: Precipitation, net water inflow and EqW during recharge period for a) SEOU site; b) BESS site and c) BEAU site.

Depth distribution of seasonal EqW

Results summarized in Table 1 for BESS site are the total EqW from the surface until the deepest station at -58m. In the BESS site, EqW deduced from gravity measurements are

Hydrol. Earth Syst. Sci. Discuss., https://doi.org/10.5194/hess-2016-355
Manuscript under review for journal Hydrol. Earth Syst. Sci.
Discussion started: 1 August 2017

Hydrology and Earth System Sciences
Open Access
Discussions

available at 5 different depths. Gravity depth profiles have nearly the same shape during recharge and discharge periods (Figure 6). During recharge period, gravity variation is equal to 9 µGal between surface and 12 m depth with a small error budget (3µGal). EqW variation is then significant at this depth with a value of 110 mm. Below 12m depth, gravity variations are not significant (2µGal, 2µGal and 0µGal respectively for the second, the third and the fourth depth stations). Error budget is ranging for 2.5 and 3.5µGal for the three depths respectively. For discharge period, time-lapse S2D gravity variation has also a value of -9µGal for the first depth with 2.5µGal of error budget. Between 12m to 23m depth, gravity variation is equal to -4µGal. Below 23m depth, gravity variation are small, 1µGal and 2µGal respectively for 23-41m and for 41-58m depth intervals.

For these two periods, EqW variations are significant only between the surface and 12m depth (~100mm). Below 12m depth most of gravity variations are not significant. Only during the discharge period, a possibly significant EqW decrease of 40 mm is measured between 12m and 23m depth.

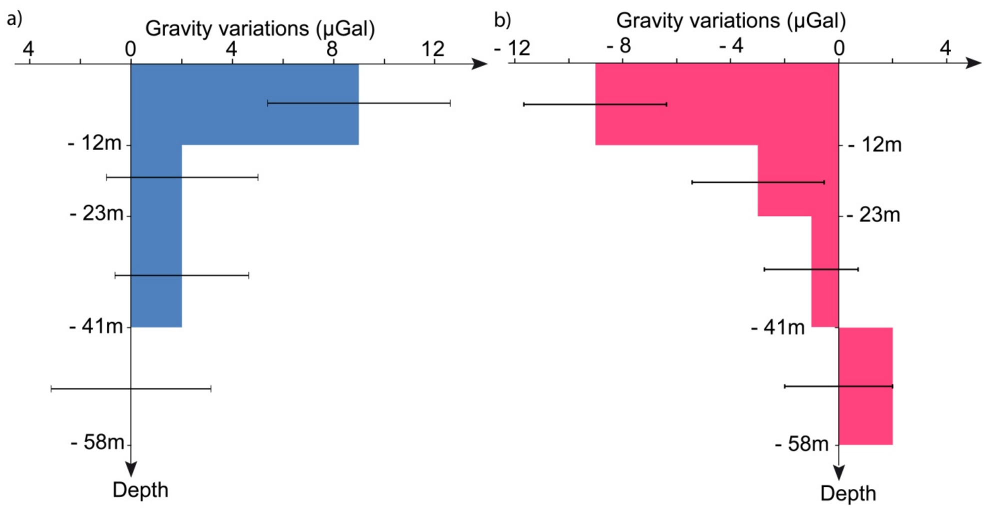

Figure 6 : S2D gravity difference function of depth at the BESS site for a) recharge period in 2010; b) and discharge period in 2011.

4) Discussion

Accuracy of S2D measurements

Gravity measurements must be very useful to determine water storage variation in unsaturated zone. In some Mediterranean areas, water storage variations lead to a maximum of 30µGal on gravity amplitude between dry and wet season (Deville et al., 2012). In our case, error budget is one order of magnitude lower than seasonal gravity amplitude. Because of an improved measurement method, we are confident that gravity differences are only due to hydrological processes.

We show using two measurement strategies that the error budget can be optimized. A long time measurements strategy (45 min per site) displays a better error budget than a short time strategy (10 min per site). However, we perform the long time strategy with a unique measurement on each station. Therefore, this strategy can be performed only if the gravimeter has a quasi-linear drift over one day. Because we are looking to a differential precision of 1 µgal, this means that the gravimeter drift curve should follow a linear trend at µgal level. In the BESS site, the coherence of the gravity measurements with respect to depth is an indirect information of the quality of the measurement. We are therefore confident that our measurements are suitable for a quantitative interpretation of differential gravity in term of water storage.

AET data has been estimated using a constant crop coefficient (k). The crop coefficient is known to be variable with time. Hence a time-constant crop coefficient leads an error on AET value. However during recharge period (i.e. autumn and winter season) evapotranspiration is low and its associated error is therefore weak. During the discharge period, the evapotranspiration plays a major role in the net water inflow error budget. The large uncertainty in the evaluation of the evapotranspiration leads a large uncertainty on the value of NWI that does not allow a reliable interpretation of the discharge period. Moreover, ambiguity remains between evapotranspiration error and water transfer below the depth of investigation.

Quantification of the epikarst water storage

The measurements done at BESS site allow for evaluating the depth distribution of the seasonal water storage variations. Both recharge and discharge periods show water storage variations in unsaturated zone mostly located within the first 12 meters (Figure 6). The seasonal water stored in BESS reaches 110 mm over this thickness. Water storage between 12 m and 55m depth is limited to a maximum value of 30mm which is the resolution of the gravity method. Therefore, water storage on this site is likely to occur in a shallow zone corresponding to the epikarst. This storage location may be enhanced by a larger porosity occurring at those depths (Williams, 2008). The unsaturated zone below (i.e., infiltration zone) may have mainly a transfer function and a small water storage capacity. Various estimations of water storage in the high porosity zone support the hypothesis of a key role of the epikarst in the seasonal water storage (Mangin, 1975; Perrin et al., 2003; Klimchouk, 2004; Williams, 2008). Spoiled structures allow water reservoir in the first meter of unsaturated zone of karst system. Following Williams (2008), epikarst thickness may vary from 10m to 30m and epikarst water storage occurs because of a strong porosity in the epikarst associated to a reduced permeability at its base. Surface to depth gravity allows a precise quantification of both storage thickness and amplitude in the unsaturated zone.

This result is important for the evaluation of the karst vulnerability. The pollution vulnerability of a karst system is complex and specify to each karst system (Marin et al., 2012; van Beynen et al., 2012). The knowledge of the amount and depth of water storage in epikarst provide new and quantitative information for the modeling of pollution infiltration. When pollution occurs, a part is immediately carried away to the spring, but another part of the pollution is stored seasonally in the first meter of unsaturated zone. The coupling between gravimetric hydrological and geochemical measurements inside the epikarst may provide significant knowledge on unsaturated aquifer pollution.

Role of lithology on epikarst water storage properties

Comparison of the ratio EqW versus NWI allows a quantification of the water storage properties of the epikarst. Seasonal water storage is measured at the three sites but with the associated ratio are significantly different. Overall, such results confirm the role of the epikarst as an active reservoir at seasonal time scale. Recharge periods of autumn and winter are weakly influenced by evapotranspiration due to low atmospheric temperature. Hence large uncertainty in the evaluation of the evapotranspiration does not critically affect the estimation of net water inflow. During recharge period, EqW increase correspond to 30% of net water inflow at SEOU and BESS sites whereas at BEAU site EqW increase is as large as 80% of NWI.

The spatial variability of the ratio EqW versus NWI can be associated to a variety of factors: lithology, thickness of the unsaturated zone or depth of the measurements, thickness of the epikarst, intensity of the fracture and alteration, among others. We discuss here the variability of seasonal epikarst water storage due to thickness of the unsaturated zone, depth of the measurements and lithology can be investigated.

Depth of gravity measurements directly defines the thickness of the investigated volume. Therefore, one could think that a thicker reservoir is associated to a larger storage. However, BESS and SEOU EqW versus NWI ratios are similar in spite of large difference of investigated thickness (~10 m for SEOU and 58 m for BESS). The thickness of the investigated zone seems therefore not to be a critical factor influencing the seasonal water storage capacity of the epikarst. This finding can be understood if most of water storage occurs in the epikarst rather than the infiltration zone as we found for BESS site.

The thickness of unsaturated zone could be correlated with its storage capacity is the storage occurs on the whole thickness. Also, one may think that a deep saturated zone could favor a fast infiltration and reduce water storage in unsaturated zone. Regarding the three sites, BESS and SEOU site have a similar EqW to NWI ratio in spite of a large difference of unsaturated thickness, which are respectively of 40m and 300m. Also, BEAU and BESS site have a similar unsaturated thickness (200-300m) but have a great difference in EqW to NWI ratio. Therefore, thickness of unsaturated zone is not a critical factor influencing seasonal water storage capacity of epikarst.

The EqW to NWI ratio from the gravity measurements is now interpreted in the terms of karst morphology or lithology. Water storage capacity seems to be largely dependent on the kind of host rock (limestone for BESS and SEOU sites and dolomite for BEAU site). Almost all the seasonal NWI is stored in the epikarst of the dolomite site. On the opposite, in the compact limestone sites, only one third of the NWI is stored. A possible explanation is that dolomite could favor seasonal water storage thanks to a developed porosity. Indeed, alteration of the dolomite favours the development of micro-porosity which in turn increases the reservoir properties of the epikarst (Quinif, 1999). Also, enlarged fractures associated to secondary porosity are filled by the residuals of dolomite alteration (sand). Structure only constituted by porosity is less permeable than a structure with clear fracture or opened fracture. By contrast, limestone is rather characterized by a small to medium micro-porosity (mudstone or packstone) drained by open fractures. Only a small part on the net water inflow can be stored in the primary and secondary porosity. As a consequence, seasonal water storage capabilities of dolomite's epikarst could be more important than those of limestone's epikarst. Unsaturated zone of dolomite karst could have a great capacitive function and a relatively limited transfer function. On the opposite, unsaturated zone of limestone karst system could have a smaller capacitive function. Some studies indicate that epikarst seems to have a large capacitive function and corresponds to a main seasonal stock of water (Klimchouk, 2004; Williams, 2008). In line with the previous study of Jacob et al. (2009), the predominant role of epikarst for water storage is confirmed by this S2D gravity survey. For dolomite rock, the capacitive function of the epikarst could retain up to 80 % of water inflow. Limestone sites reveal to be less efficient for epikarst water storage. Indeed, 60% of NWI is transferred in the infiltration and/or in the saturated zone where storage could occur. However, porosity is highly dependent of the type of limestone and our two sites have compact limestone. We also acknowledge also that the deep saturated water storage cannot be measured from S2D gravity measurements except if the survey includes surface absolute gravimeter measurements.

Capacitive and transmissive reservoir properties

Surface time-lapse gravity survey highlights only storage properties of karst system (Deville et al., 2012). Surface time gravity measurements do not allow an interpretation of water transfer properties. However, when gravity time-series are associated to a hydrological model to correct surface effects (topography and building umbrella effect), one can determine water transfer properties. But such a study requires gravity measurements with time-spacing lower than two months which is clearly not the case in the present study. However, due to time-lapse

Hydrology and Earth System Sciences
Open Access
EGU
Discussions

S2D measurements, it is possible to deduce partially water transfer properties. As gravity measurements are repeated every 6 months, the ratios EqW versus NWI indicate if the water time transfer is larger than 6 months (or not). During the recharge period, the epikarst reservoir is filled by water fluxes from surface. As large seasonal water storage are observed such in BEAU, the transfer time of the epikarst reservoir should excess 6 months. As almost no inter-annual cycle has been observed (Deville et al., 2012) on Durzon karst system from surface absolute gravity measurements, the transfer time should be less than one year. The range of transfer time is also in accordance with the model result obtained on Durzon karst system (Deville et al., 2012). A long transfer time of the epikarst reservoir to the infiltration zone of about 6-12 months can be proposed for altered dolomite karst with a lack of high transmissive fractures. On the opposite, only a small part of the NWI is stored in the limestone epikarst (BESS, SEOU) after the recharge period. A short transfer time (< 6 months) in the limestone karst is therefore necessary and can be due to open fracture as observed in surface. At SEOU site, Chevalier (1988) shown with the analysis of spring during flood events that water transfer is fast between surface to spring (few days) and the major part of net water inflow is retrieved some days after rain at the spring.
With an exponential decrease model of the epikarst water, a mean life-time of 3.5 and 13 months for the short (limestone) and long (dolomite) transfer time can be estimated. One can finally look at the SEOU recharge 2010 survey which has an abnormal high EqW increase (table 2). The measure was done only a few days (one day) after a heavy rainfall and a major part of water from fast transfer is probably still present in the unsaturated zone.

5) Conclusion and perspective

Our time-lapse S2D methodology uses in-situ measurements in karstic caves during the extrema of the seasonal climatic cycle. The large volume investigated by gravity measurements scales to the depth of investigation which is here 10-50 m. This leads to investigate medium heterogeneity over this spatial scale. The three studied areas display different morphology, lithology and climate. However, significant seasonal water storage is always present. Physical reservoir properties and their difference from site to site have been estimated. We highlight a different capacitive function between the two sites located in limestone with respect to the one embedded in a dolomite environment. One explanation of these specific behaviors could be a petro-physical difference between limestone and dolomite. The thickness of the epikarst has been estimated in the BESS site thanks to gravity stations regularly spaced in depth. The seasonal water storage mostly occurs in the 12 first upper meters, possibly matching the high porosity zone of the epikarst. The infiltration zone below 12 m seems to have only a transfer function. Therefore, even in a relatively shallow epikarst, seasonal water storage is never negligible (about 30% of net water inflow).

No relation between seasonal water storage amplitude and morphology of karst system (i.e. unsaturated zone thickness) has been observed. By contrast, the seasonal water storage (EqW) versus net water inflow (NWI) ratio seems to be dependent from the lithology. Especially, the alteration of the dolomite seems to enhance storage properties of the epikarst. Dolomite's epikarst seems to a greater capacitive function than limestone's epikarst.

The transmissive function of the epikarst can be partially estimated from the gravity water storage estimations. Long transfer time in the dolomite (> 6 months) and short in the limestone (< 6 months) are observed. The study of the karst transfer function cannot be done directly from surface gravity measurements and is a clear advantage of S2D setup. The addition of an absolute gravity monitoring at the surface allow to estimate the water storage both between the surface and depth but also below the depth measurement and give constrain on the infiltration / saturated zone.

Since the paper focus only on three sites, the results should be compared with other measurements in various karst systems to analyze more rigorously the impact of the fracture, the alteration and the lithology. Moreover, gravity observations should be combined with in-situ flux such as seepage or geophysical such as Magnetic Resonance Sounding measurements (Mazzilli et al., 2016) in order to study the relation between water storage, total water stock and local transfer properties. These collocated measurements should lead to a better knowledge of unsaturated zone properties and processes. Transfer and storage modeling could then be constrained at an intermediate scale (~100m). In order to investigate epikarst time-dependent properties, continuous gravity observatory coupled with local evapotranspiration measurements are mandatory (Fores et al., 2017).

Acknowledgments:

The project is part of the HydroKarst G^2 project from 2009 to 2013 funded by the French Agence Nationale de la Recherche (ANR). Gravity surveys were part of the OSU OREME funded by the Institut de Recherche pour le Développement (IRD) and the Institut National des Sciences de l'Univers (INSU) and of SNO-SOERE H+ (INSU). The Scintrex CG5 relative gravimeter was loaned by the Gravity Mobile facility (GMOB) of RESIF-INSU. We would also like to acknowledge the farmer of SEOU and BESS to let us access the caves.

Al-fares, W., M. Bakalowicz, R. Guérin & M. Dukhan, 2002. Analysis of the karst aquifer structure of the Lamalou area (Hérault, France) with ground penetrating radar. Journal of Applied Geophysics 51: 97-106.

Allen, G. A., L. S. Pereira, D. Raes & M. Smith, 1998. Crop evapotranspiration - Guidelines for computing crop water requirements. Rome, FAO-Food and Agriculture Organization of the United Nations.

Bakalowicz, M., 2005. Karst groundwater: a challenge for new resources. Hydrogeology Journal 13(1): 148-160.

Batiot, C., C. Emblanch & B. Blavoux, 2003. Carbone Organique Total (COT) et Magnésium (Mg2+) : deux traceurs complémentaires du temps de séjour dans l'aquifère karstique. C. R. Geoscience 335: 205-214.

Beilin, J., 2006. Apport de la gravimétrie absolue à la réalisation de la composante gravimétrique du Réseau Géodésique Français, Institut Géographique National.

Boinet, N., 1999. Exploitation de la fracturation d'un massif par la karstification : exemple de Causse de l'Hortus (Hérault, France). Geodinamica Acta 12(3-4): 237-247.

Boinet, N., 2002. Inventaire spéléologique du Causse de l'Hortus-Tome 4.

Bonnet, M., A. Lallemand-Barres, D. Thiery, H. Bonin & H. Paloc, 1980. Etude des mécanismes de l'alimentation d'un massif karstique à travers la zone non saturée. Application au massif de l'Hortus. S. g. N.-S. H. Rapport du BRGM.

Bonvalot, S., D. Remy, C. Deplus, M. Diament & G. Gabalda, 2008. Insights on the March 1998 eruption at Piton de la Fournaise volcano (La Reunion) from microgravity monitoring. Journal of Geophysical Research-Solid Earth 113(B5).

Budetta, G. & D. Carbone, 1997. Potential application of the Scintrex CG-3M gravimeter for monitoring volcanic activity; results of field trials on Mt. Etna, Sicily. Journal of Volcanology and Geothermal Research 76(3-4): pp. 199-214.

Chevalier, J., 1988. Hydrodynamique de la zone non saturée d'un aquifère karstique : Etude expérimentale. Site du Lamalou-Languedoc, Université Montpellier 2: 195p.

Civiate, M. & F. Mandel, 2008. La mesure de hauteurs de précipitations - Fiche descriptive sur les instruments de mesure météorologique -Version 1.0. Météo-France.

Davis, K., Y. Li & M. Batzle, 2008. Time-lapse gravity monitoring: A systematic 4D approach with application to aquifer storage and recovery. Geophysics 73(6).

Deville, S., T. Jacob, J. Chery & C. Champollion, 2012. On the impact of topography and building mask on time varying gravity due to local hydrology Geophysical Journal International In press.

Durand, V., 1992. Structure d'un massif karstique. Relations entre déformations et facteurs hydrométéorologiques, Causse de l'Hortus - sites des sources du Lamalou (Hérault), Université Montpellier II. PhD Thesis.

Emblanch, C., C. Zuppi, J. Mudry, B. Blavoux & C. Batiot, 2003. Carbon 13 of TDIC to quantify the role of the unsaturated zone: the example of the Vaucluse karst systems (Southeastern France). Journal of Hydrology 279(1-4): 262-274.

Fleury, P., M. Bakalowicz & M. Becker, 2007. Characterising a karst system with a submarine spring: the example of La Mortola (Italy). Comptes Rendus - Academie des sciences. Geoscience 339(6): pp. 407-417, doi:410.1016/j.crte.2007.1004.1004

Flury, J.; Peters, T.; Schmeer, M.; Timmen, L.; Wilmes, H.; Falk, R., 2007. Precision gravimetry in the new Zugspitze gravity meter calibration system; Proceedings of the 1st International Symposium of the International Gravity Field Service, Istanbul 2006, Harita Dergisi, Special Issue, Nr. 18, pp 401-406, ISSN 1300-5790, 2007

Fores, B., Champollion, C., Le Moigne, N., Bayer, R., Chéry, J. (2017a). Assessing the precision of the iGrav superconducting gravimeter for hydrological models and karstic hydrological process identification. Geophysical Journal International. 208(1), 269-280.

Harnisch, G. & M. Harnisch, 2006. Hydrological influences in long gravimetric data series. Journal of Geodynamics 41: 276-287.

Hu, C., Y. Hao, T. J. Yeh, B. Pang & Z. Wu, 2008. Simulation of spring flows from a karst aquifer with an artificial neural network. Hydrological Processes 22: 596-604.

Hwang, C., C. G. Wang & L.-H. Lee, 2002. Adjustment of relative gravity measurements using weighted and datum-free constraints. Computers & Geosciences 28(9): pp. 1005-1015.

Jacob, T., 2009. Apport de la gravimétrie et de l'inclinométrie à l'hydrogéologie karstique. Geosciences Montpellier. Montpellier, Université des Sciences et Technologies.

Jacob, T., R. Bayer, J. Chery, H. Jourde, N. Le Moigne, J. P. Boy, J. Hinderer, B. Luck & P. Brunet, 2008. Absolute gravity monitoring of water storage variation in a karst aquifer on the Larzac plateau (Southern france). J.of Hydrology 359(1-2): 105-117, doi:110.1016/j.jhydrol.2008.1006.1020.

Jacob, T., R. Bayer, J. Chery & N. Le Moigne, 2010. Time-lapse microgravity surveys reveal water storage heterogeneity of a karst aquifer. Journal of Geophysical Research-Solid Earth 115.

Jacob, T., J. Chery, R. Bayer, N. Le Moigne, J. P. Boy, P. Vernant & F. Boudin, 2009. Time-lapse surface to depth gravity measurements on a karst system reveal the dominant role of the epikarst as a water storage entity. Geophys. J. International 177: 347-360 doi: 310.1111/j.1365-1246X.2009.04118.x.

Klimchouk, A., 2004. Towards defining, delimiting and classifying epikarst: Its origin, processes and variants of geomorphic evolution. Proc. of the symposium held October 1 through 4, 2003 Sheperdstown, West Virginia, USA. Karst Water Institute special publication, Epikarst 9(1): 23-25.

Lastennet, R. & J. Mudry, 1997. Role of karstification and rainfall in the behavior of a heterogeneous karst system. Environmental Geology 32(2): 114-123.

Legchenko, A., J. M. Baltassat, A. Beauce & J. Bernard, 2002. Nuclear magnetic resonance as a geophysical tool for hydrogeologists. Journal of Applied Geophysics(50): pp. 21-46.

Mangin, A., 1975. Contribution à l'étude hydrodynamique des aquifères karstiques, Université de Dijon. Ph.D. Thesis: 124.

Marin, A. I., N. Doerfliger & B. Andreo, 2012. Comparative application of two methods (COP and PaPRIKa) for groundwater vulnerability mapping in Mediterranean karst aquifers (France and Spain). Environmental Earth Sciences 65(8): 2407-2421.

Mazzilli, N., Boucher, M., Chalikakis, K., Legchenko, A., Jourde, H., & Champollion, C. 2016. Contribution of magnetic resonance soundings for characterizing water storage in the unsaturated zone of karst aquifers. Geophysics, 81(4), WB49-WB61.

Merlet, S., A. Kopaev, M. Diament, G. Geneves, A. Landragin & F. Pereira Dos Santos, 2008. Micro-gravity investigations for the LNE watt balance project. Metrologia 45: 265-274 doi: 210.1088/0026-1394/1045/1083/1002.

Perrin, J., P. Jeannin & F. Zwahlen, 2003. Epikarst storage in a karst aquifer: a conceptual model based on isotopic data, Milandre test site, Switzerland. Journal of Hydrology 279: 106-124.

Pfeffer, J., C. Champollion, G. Favreau, B. Cappelaere, J. Hinderer, M. Boucher, Y. Nazoumou, M. Oï, M. Mouyen, C. Henri, N. Le Moigne, S. Deroussi, J. Demarty, N. Boulain, N. Benarrosh, O. Robert, 2013. Evaluating surface and subsurface water storage variations at small time and space scales from relative gravity measurements in semiarid Niger, Water Resour. Res., 49, 3276–3291, doi:10.1002/wrcr.20235.

Pinault, J. L., V. Plagnes, L. Aquilina & M. Bakalowicz, 2001. Inverse modeling of the hydrological and the hydrochemical behavior of hydrosystems; characterization of karst system functioning. Water Resources Research 37: 2191-2204.

Quinif, Y., 1999. Fantômisation, cryptoaltération et altération sur roche nue, le triptyque de la karstification. Actes du colloque européen Karst-99: 159-164.

Réméniéras, G., 1986. L'hydrologie de l'ingénieur. Paris, EDF et Eyrolles ed.

Schwiderski, E. W., 1980. Ocean tides, II: A hydrodynamic interpolation model. Marine Geodesy 3: pp. 219-255.

Scintrex limited, 2006. CG5 Scintrex autograv system Operation Manual. Concord, Ontario, Scintrex Limited.

SIE Rhône-Méditerranée, e.-f. (2011). Fiche de caractérisation des masses d'eau souterraine : Calcaires et marnes Causses et avant-Causses du Larzac sud, Campestre, Blandas, Séranne,. from http://www.rhone-mediterranee.eaufrance.fr/.

Tamura, Y., 1987. A harmonic development of the tide generating potential. Bull. d'Inf. Marées Terr. 99.

Turc, L., 1961. Evaluation des besoins en eau d'irrigation, évapotranspiration potentielle. Annales Agronomiques 12(1): 13-49.

Valois, R., 2011. Caractérisation structurale de morphologies karstiques superficielles et suivi temporel de l'infiltration à l'aide des méthodes électriques et sismiques. Sisyphe. Paris, Université Pierre et Marie Curie: 244.

van Beynen, P. E., M. A. Niedzielski, E. Bialkowska-Jelinska, K. Alsharif & J. Matusick, 2012. Comparative study of specific groundwater vulnerability of a karst aquifer in central Florida. Applied Geography 32(2): 868-877.

Van Camp, M., P. Meus, Y. Quinif, O. Kaufman, M. Van Ruymbeke, M. Vandiepenbeeck & T. Camelbeek, 2006a. Karst aquifer investigation using absolute gravity. Eos Transactions 87(30): pp. 298.

Van Camp, M., M. Vanclooster, O. Crommen, T. Petermans, K. Verbeeck, B. Meurers, T. van Dam & A. Dassargues, 2006b. Hydrogeological investigations at the Membach station, Belgium, and application to correct long periodic gravity variations. Journal of Geophysical Research 111: B10403.

Wenzel, H.-G., 1996. The Nanogal software: earth tide data processing package ETERNA 3.30. Bulletin d'Informations des Marees Terrestres 124: 9425–9439.

Williams, P. W., 2008. The role of the epikarst in karst and cave hydrogeology: a review. International Journal of Speleology 37(1): 1-10.

Wu, J., A. G. Journel & T. Mukerji, 2006. Establishing spatial pattern correlations between water saturation time-lapse and seismic amplitude time-lapse. Journal of Canadian Petroleum Technology 45(11): 15-20.

Hydrol. Earth Syst. Sci. Discuss., https://doi.org/10.5194/hess-2016-355
Manuscript under review for journal Hydrol. Earth Syst. Sci.
Discussion started: 1 August 2017

Zhang, Z., X. Chen, A. Ghadouani & S. Peng, 2011. Modelling hydrological processes influenced by soil, rock and vegetation is a small karst basin of southwest China. Hydrological Processes 25: 2456-2470.

Hydrol. Earth Syst. Sci. Discuss., https://doi.org/10.5194/hess-2016-355
Manuscript under review for journal Hydrol. Earth Syst. Sci.
Discussion started: 1 August 2017

Hydrology and Earth System Sciences
Open Access
Discussions

Annex 1 : *Results of the least square inversion for each site and each time periods. Results at BESS site is represented for each thickness. Occup. Stands for the number of gravity measurements at the reference gravity points depending on the strategy (long or short).*

Site	***Date***	***Occup.***	***Calibration correction factor***	***ΔgS2D (mGal)***	***σ STD (mGal)***
SEOU	t_1 : 24/02/2010	4 to 5	0.999377	-3.897	0.0014
	t_2 : 26/08/2010	4 to 5	0.999337	-3.914	0.0036
	t_3 : 07/10/2010	1 to 2	0.999337	-3.910	0.0014
	t_4 : 03/05/2011	1 to 2	0.999569	-3.906	0.0014
	t_5 : 13/09/2011	1 to 2	0.999569	-3.909	0.0014
BESS (0,-12m)	t_1 : 01/03/2010	4 to 5	0.999377	-1.523	0.0014
	t_2 : 24/08/2010	4 to 5	0.999337	-1.537	0.0028
	t_3 : 01/10/2010	1 to 2	0.999337	-1.531	0.0014
	t_4 : 05/05/2011	1 to 2	0.999569	-1.528	0.0022
	t_5 : 06/09/2011	1 to 2	0.999569	-1.537	0.0014
BESS (-12,-23m)	t_1 : 01/03/2010	4 to 5	0.999377	-1.320	0.0014
	t_2 : 24/08/2010	4 to 5	0.999337	-1.320	0.0022
	t_3 : 01/10/2010	1 to 2	0.999337	-1.322	0.0014
	t_4 : 05/05/2011	1 to 2	0.999569	-1.317	0.0020
	t_5 : 06/09/2011	1 to 2	0.999569	-1.320	0.0014
BESS (-23,-41m)	t_1 : 01/03/2010	4 to 5	0.999377	-1.724	0.0022
	t_2 : 24/08/2010	4 to 5	0.999337	-1.724	0.0022
	t_3 : 01/10/2010	1 to 2	0.999337	-1.728	0.0014
	t_4 : 05/05/2011	1 to 2	0.999569	-1.726	0.0010
	t_5 : 06/09/2011	1 to 2	0.999569	-1.727	0.0014
BESS (-41,-58m)	t_1 : 01/03/2010	4 to 5	0.999377	-1.277	0.0028
	t_2 : 24/08/2010	4 to 5	0.999337	-1.275	0.0028
	t_3 : 01/10/2010	1 to 2	0.999337	-1.272	0.0014
	t_4 : 05/05/2011	1 to 2	0.999569	-1.275	0.0014
	t_5 : 06/09/2011	1 to 2	0.999569	-1.273	0.0014